Physics and Imaging in Radiation Oncology 8 (2018) 17–22

Contents lists available at ScienceDirect

Physics and Imaging in Radiation Oncology

journal homepage: www.elsevier.com/locate/phro

Original Research Article

Stereotactic body proton therapy for liver tumors: Dosimetric advantages and their radiobiological and clinical implications

W. Tristram Arscott[a,1], Reid F. Thompson[b,1], Lingshu Yin[a], Brendan Burgdorf[a], Maura Kirk[a], Edgar Ben-Josef[a,*]

[a] Department of Radiation Oncology, Hospital of the University of Pennsylvania, United States
[b] Department of Radiation Medicine, Oregon Health & Science University, Portland VA Healthcare System, United States

ARTICLE INFO

Keywords:
Proton SBRT
Liver SBRT
NTCP

ABSTRACT

Background and Purpose: Photon Stereotactic Body Radiotherapy (SBRT) for primary and metastatic tumors of the liver is challenging for larger lesions. An *in silico* comparison of paired SBRT and Stereotactic Body Proton Therapy (SBPT) plans was performed to understand the potential advantages of SBPT as a function of tumor size and location.

Methods and materials: Theoretical tumor volumes with maximum diameter of 1–10 cm were contoured in the dome, right inferior, left medial, and central locations. SBRT and SBPT plans were generated to deliver 50 Gy in 5 fractions, max dose < 135%. When organs-at-risk (OAR) constraints were exceeded, hypothetical plans (not clinically acceptable) were generated for comparison. Liver normal tissue complication probability (NTCP) models were applied to evaluate differences between treatment modalities.

Results: SBRT and SBPT were able to meet target goals and OAR constraints for lesions up to 7 cm and 9 cm diameter, respectively. SBPT plans resulted in a higher integral gross target dose for all lesions up to 7 cm (mean dose 57.8 ± 2.3 Gy to 64.1 ± 2.2 Gy, $p < 0.01$). Simultaneously, SBPT spared dose to the uninvolved liver in all locations (from 11.5 ± 5.3 Gy to 8.6 ± 4.4 Gy, $p < 0.01$), resulting in lower NTCP particularly for larger targets in the dome and central locations. SBPT also spared duodenal dose across all sizes and positions (from 7.3 ± 1.1 Gy to 1.1 ± 0.3 Gy, $p < 0.05$).

Conclusion: The main advantages of SBPT over SBRT is meeting plan goals and constrains for larger targets, particularly dome and central locations, and sparing dose to uninvolved liver. For such patients, SBPT may allow improvements in tumor control and treatment safety.

1. Introduction

Stereotactic body radiotherapy (SBRT) is being increasingly used in primary and metastatic liver cancers. SBRT can provide excellent local tumor control with minimal toxicity [1–3], and is being evaluated as an alternative or adjuvant to other therapies as a bridge to transplant in eligible patients [4]. SBRT is also being incorporated into treatment paradigms for oligometastatic disease [5].

An ongoing challenge in liver SBRT planning is ensuring delivery of sufficient dose for tumor control with high enough conformality to spare dose to the uninvolved liver to preserve organ function. Despite technical advances in photon-based planning, delivering tumoricidal doses to larger (> 6 cm) lesions remains difficult [6–8]. Ongoing clinical practice and studies such as NRG/RTOG 1112 (NCT01730937) allow treating lesions up to 10 cm with photon SBRT, however this only remains achievable by significantly compromising prescription dose. GTV dose influences local control rates in both primary liver cancers and metastases, and while some studies have not shown a decrement in local control when prescription dose must be compromised to meet OAR constraints [1], others have demonstrated inferior local control [2,3,9–12]. Because of its finite range and consequent lower integral dose deposition, proton therapy may enable SBRT for larger tumor volumes without compromising target coverage or violating OAR constraints. Indeed, proton based SBRT programs are developing for new disease sites to capitalize its dosimetric advantages of the proton Bragg peak, and a few clinical trials (NCT01697371 [liver metastases],

* Corresponding author at: Department of Radiation Oncology, University of Pennsylvania, Perelman Center for Advanced Medicine, 4 West, Room 316, 3400 Civic Center Blvd., Philadelphia, PA 19104, United States.
E-mail address: edgar.ben-josef@uphs.upenn.edu (E. Ben-Josef).
[1] Equal contributions.

https://doi.org/10.1016/j.phro.2018.11.004
Received 6 June 2018; Received in revised form 13 November 2018; Accepted 13 November 2018

NCT03159676 [prostate]) have opened. A number of analyses have been published, showing improved OAR dose distribution by replanning photon hypofractionated regimens with protons [13,14]. However, a systematic investigation of location and size of the target and their impact on the hypothesized therapeutic gain with protons has not yet been reported.

To address this gap in knowledge, we performed an in-depth *in silico* analysis of paired photon SBRT and stereotactic body proton therapy (SBPT) plans for theoretical targets, with maximum diameters ranging from 1 cm to 10 cm in four different locations within the liver.

2. Methods

2.1. Target generation

Target volumes were contoured as isotropic expansions of a 1 cm-diameter target up to 10 cm diameter, cropped to remain within the liver contour on axial slices in 4 different locations within the liver: dome, right inferior, left medial, central (positions A, B, C and D, corresponding approximately to liver segments 8, 6, 4, and 5, respectively; see Supplement A). Thus, a total of 40 "virtual" lesions were generated and used for dosimetric evaluations performed in this investigation, and these volumes were considered the gross target volume (GTV). A 0.5 cm expansion was added for the planning target volume (PTV). Regional organs-at-risk (OARs) were contoured, including stomach, duodenum, small bowel, large bowel, lungs, kidneys, heart/pericardium, chest wall/rib, skin, spinal cord, with liver minus GTV referred to as "liver" herein.

2.2. Treatment planning

Photon volumetric modulated arc therapy (VMAT) and proton pencil beam scanning (PBS) plans were generated in Eclipse, version 13.7 (Varian Ltd, Palo Alto, California), for each of the 10 target sizes in the 4 locations within the liver (n = 80 plans), with a prescription of 50 Gy in 5 fractions at 10 Gy per fraction. Mean liver dose (liver – GTV) was constrained to < 14 Gy, and 700 cm^3 to < 15 Gy as clinically verified for safety [15–18] (see Table 1 for additional OAR constraints). If the chest wall was the only constraint violation, this was considered a variation acceptable as long as all other OAR constraints were met. For photon SBRT VMAT planning, coplanar and non-coplanar arcs were used, optimized separately for each target to maximally avoid OARs. Linac used for planning was a Varian Truebeam with standard millennium MLCs. For SBPT planning, a PBS universal nozzle gantry was utilized, which provides a 100–230 MeV beam (IBA Ltd, Leuven, Belgium) and uses a range shifter with minimal air gap for shallow target coverage. The range of energy layer spacing used was between 4 mm and 8 mm (4 times the energy spread sigma in depth) depending on the energy of the beam used (sigma sizes vary between 1 mm for ~100 MeV beams to 2 mm for ~200 MeV beams). A fixed spot spacing of 0.5 cm was used within each layer. Multiple non-coplanar beams (minimum two for small targets, up to four for larger targets) were oriented to minimize overlap (minimum 60° separation). Proton plans were calculated by single field uniform dose optimization, with a relative biologic effectiveness correction factor of 1.1. Both modalities used a calculation grid size of 2.5 mm. For both photon and proton SBRT plans, optimization was performed such that 95% of the PTV received 100% of the prescription dose, while achieving OARs. GTV doses were pushed as high as achievable while meeting OAR constraints and respecting a 135% maximum hot spot limit. In cases where all OARs could not be met, focus was placed on target coverage and maximal liver sparing for optimization. All plans were generated, jointly, by two physicists (M.K. and B.B.), and each plan was created *de novo*, without explicit reference to any planning parameters or dosimetry from other lesions or locations.

Table 1
Planning constraints.

Organ at risk	Volume (cm^3)	Volume maximum (Gy)	Point dose maximum (Gy)
Spinal cord	0.1	25	30
	< 0.35	23	
	< 1.2	14.5	
Liver – GTV	700	15	
	Mean < 14 Gy		
Stomach	0.1	27.5	32
	< 10	18	
Duodenum	0.1	30	32
	< 5	18	
	< 10	12.5	
Esophagus	< 5	19.5	35
Small bowel	< 5	19.5	35
Large bowel	< 20	25	38
Lung total	1500	12.5	
Lung total	1000	13.5	
Kidney total	200	17.5	
Heart/pericardium	< 15	32	38
Chest wall/rib	< 30	30	43
Skin	< 10	36.5	39.5

2.3. Data and statistical analysis

Dose-volume histogram (DVH) data for all plans were exported from Eclipse and analyzed using the RadOnc package (1.1.3) for R (3.4.0) [19]. We assessed standard dosimetric parameters including duodenum, heart/pericardium, liver, stomach, small bowel, chest wall/skin. Generalized equivalent uniform dose (gEUD) models were applied for the GTVs to summarize respective DVHs as single biologically weighted values (tissue-specific parameter a = -5 and a = -15, as in prior work) [20]. Linear quadratic extrapolated dose conversion was used to express integral dose in 2 Gy equivalents for comparison (LQED2), assuming α/β ratio of 10 Gy for GTV and 3 Gy for OARs. Normal tissue complication probability (NTCP) was computed using the Lyman-Kutcher-Burman model (n = 0.97 and m = 0.12 [21]), applied to biologically-corrected DVH data (2 Gy/fraction equivalent dose), α/β ratio of 2.5 Gy. Wilcoxon signed-rank test methodology with $\alpha = 0.05$ was used to compare target and OAR parameters across target sizes.

3. Results

3.1. Clinical deliverability of SBRT plans

SBRT met constraints and would be considered acceptable for patient treatment for GTV diameters up to 7 cm, 5 cm, 6 cm, and 3 cm for positions A, B, C and D, respectively. SBPT met constraints for larger targets; up to 9 cm, 7 cm, 6 cm, and 7 cm for these same positions, respectively. Limitations of deliverable plans were location-dependent based on violation of OAR constraints (Table 2 [first constraints not met], Supplement B [constraints not met at each target size/location]). Generally, SBPT met liver constraints for larger tumor volumes, sparing a greater volume of uninvolved liver compared with SBRT (915 ± 34 cm^3 v. 856 ± 38 cm^3, $p < 0.01$, across all target sizes and locations). Positions A and D were dosimetrically limited at the largest volumes principally due to violation of the liver constraints, while positions B and C were constrained by small bowel, duodenum, and stomach.

3.2. Target coverage

SBPT had superior GTV coverage compared to SBRT across all tumor volumes, as measured by Dmean, gEUD (a = -5), gEUD (a = -15), and D95%, with an average increase of 4.4 ± 0.7 Gy [13.6%], 4.4 ± 0.7 Gy [13.7%], 4.4 ± 0.7 Gy [13.8%], and 4.4 ± 0.7 Gy

Table 2
Maximum target size achievable with each treatment modality, and the constraint(s) not met during planning.

	Photon		Proton	
	Target size limit (cm)	Constraint(s) not met	Target size limit (cm)	Constraint(s) not met
Dome	7	Liver-GTV	9	Liver-GTV, chest wall (at 10 cm)
Right Inferior	5	Bowel, duodenum, liver-GTV (at > 8 cm)	7	Bowel, duodenum, liver-GTV (at 10 cm)
Left medial	6	Duodenum, esophagus, heart/pericardium, liver-GTV (at ≥ 8 cm), stomach	6	Duodenum, heart/peri-cardium (≥ 9 cm), liver-GTV (at 10 cm), stomach
Central	3	Duodenum, liver (> 7 cm)	7	Chest wall (at ≥ 8 cm), liver-GTV

Table 3
Additional GTV dose coverage with protons.

Position	Dmean (Gy)	gEUD(-5) (Gy)	gEUD(−1 5) (Gy)	D95% (Gy)
Dome*	7.6 ± 0.9	7.7 ± 0.9	7.7 ± 0.9	8.0 ± 0.8
Right inferior*	2.4 ± 1.7	2.4 ± 1.7	2.0 ± 1.7	3.0 ± 1.3
Left medial*	2.8 ± 0.8	2.9 ± 0.8	3.0 ± 0.9	3.6 ± 1.0
Central*	4.5 ± 1.5	4.7 ± 1.4	4.8 ± 1.4	5.8 ± 1.2
Average	4.4 ± 0.7	4.4 ± 0.7	4.4 ± 0.7	5.1 ± 0.6

Values represent average difference (proton minus photon) across all sizes ± standard error. *Differences were statistically significant (p < 0.05) for targets up to 7 cm. Differences were not significant for targets > 7 cm.

[14.6%], respectively ($p < 0.05$ for all; Table 3). The greatest improvement in target coverage was in the hepatic dome (position A) (mean increase in GTV Dmean 7.6 ± 0.9 Gy, $p < 0.01$; and similar values when applying gEUD and D95% calculations; Table 3 and Supplement C). We also compared standardized dose, confirming that SBPT delivered higher average LQED2 compared to SBRT (107.0 ± 1.1 Gy v. 94.1 ± 0.9 Gy, $p < 0.01$), with comparable differences when applying gEUD (Supplements D and E).

For other positions in the liver, SBPT exhibited more variable dosimetric outcomes. Lesions in the right inferior liver (position B) had higher Dmean, gEUD and D95% up to 6 cm in size, but relatively reduced coverage for lesions > 6 cm (average decrease Dmean 4.0 ± 0.5 Gy, $p < 0.01$) in order to meet OAR constraints (Table 3, and Supplements G and H). At position C (left medial), the average increase in Dmean was 2.8 ± 0.8 Gy ($p < 0.01$), and the LQED2 to GTV across all target sizes was 102.0 ± 2.2 Gy for SBPT compared to 97.2 ± 1.6 Gy for SBRT (average of Dmean, gEUD, and D95%; $p < 0.01$; Table 3, and Supplements I and J), but for larger sizes (8–10 cm) the dose was similar (93.2 ± 0.7 Gy and 93.2 ± 1.8 Gy, respectively). At position D (central), the average increase in GTV Dmean was 4.5 ± 1.5 Gy across all target sizes ($p < 0.01$; Table 3 and Supplement K, and dose in LQED2 was 103.5 ± 2.1 Gy in proton plans versus 95.8 ± 0.6 Gy in photon plans ($p < 0.01$; Supplement L), though this gain was lost at the 9 and 10 cm target sizes.

3.3. Liver sparing

At position A, a greater volume of liver was spared in all SBPT compared to SBRT plans (mean increase in volume of liver receiving < 15 Gy of 68 ± 11 cm^3, $p < 0.01$), however the difference was more pronounced with increasing size ≥ 7 cm (mean difference 90 ± 10 cm^3, $p < 0.01$) (Fig. 1A and Table 4). SBPT plans met volumetric liver constraints for larger lesions than SBRT (up to 9 cm v. 7 cm, Fig. 1A, Table 2 and Supplement F). The mean liver dose was also lower in all SBPT plans (average decrease of 3.5 ± 0.6 Gy, $p < 0.01$), particularly for target diameters ≥ 7 cm (average decrease of 4.9 ± 0.9 Gy, $p = 0.01$). Fig. 1B examines the relationship between the volume of liver receiving < 15 Gy and mean liver dose. It shows that SBPT maintained both a lower mean liver dose and greater volume of uninvolved liver receiving < 15 Gy compared to SBRT across all target sizes. In addition, it shows that in photon plans there is a more linear relationship between mean liver dose and the volume receiving < 15 Gy, whereas in proton plans, in cases with similar volume receiving < 15 Gy, there is a greater reduction in mean liver dose.

At position A, SBPT and SBRT NTCP was similar (< 5%) for target sizes up to 5 cm. For larger targets however, SBPT resulted in progressively lower NTCP compared to SBRT (14% v. 99% for 10 cm targets, Fig. 2A).

Position D in the liver showed a similar relationship of target diameter to liver sparing as position A, with SBPT demonstrating a lower dose to the liver across all sizes (mean difference 2.7 ± 0.4 Gy, $p < 0.05$; Table 4, and Supplements Q and R). Volumetric constraint of 700 cm^3 < 15 Gy was met for target diameters up to 7 and 6 cm in SBPT and SBRT, respectively. NTCP was similar at position D for both photon and proton plans up to 5 cm (< 10%), however SBPT showed improved NTCP compared to SBRT for larger targets, albeit to a lesser degree than position A (Fig. 2D). At position B and C, SBPT reduced mean liver dose compared to SBRT (decreases of 2.3 ± 0.6 Gy and 3.1 ± 0.4 Gy, respectively, $p < 0.01$, Table 4, and met volumetric constraints for larger sizes (9 cm v. 7 cm at both positions, Supplements M–P). NTCP calculations at positions B and C were < 10% in all proton plans, even at the largest target sizes. SBRT NTCP increased with targets ≥ 7 cm at position B (Fig. 2B), while remaining < 10% across all sizes at position C (Fig. 2C).

3.4. Duodenum sparing

Across all sizes, the most dramatic dose sparing to the duodenum was for SBPT at positions A and D (90% and 89% lower mean dose, respectively, compared with SBRT; $p = 0.03$, $p < 0.01$; Supplements S and V, respectively). SBPT met all constraints for larger targets than SBRT (up to 9 cm and 8 cm v. 7 cm and 4 cm, for positions A and D, respectively). At position B, proton and photon plans violated duodenum constraints at target diameters of 8 cm and 5 cm, respectively, with SBPT averaging 75.5% lower mean dose across all sizes ($p < 0.01$) (Supplement T). At position C, the duodenum constraints were violated in both plans once target diameters reached 7 cm; with a mean reduction of 15.9% in SBPT v. SBRT ($p = 0.04$) (Supplement U).

3.5. Other OAR constraints

The dose to esophagus, heart/pericardium, small/large bowel, stomach, and chest wall/skin were also evaluated, and constraint compliance as a function of target size and position is shown in Supplement B. At position A, SBPT met stomach constraints for larger targets than SBRT (10 cm v. 7 cm, respectively). At position B, SBPT met large and small bowel dose constraints for larger targets than SBRT (7 cm and 7 cm v. 5 cm and 6 cm, respectively). At position C, photon plans violated small bowel, large bowel, stomach, esophagus, and heart/pericardium at 10, 10, 7, 9 and 8 cm, respectively. Proton plans violated those constraints at the same sizes, other than the heart/pericardium which was violated once target diameters reached 9 cm. At position D, protons violated the point dose max (38 Gy) for the large bowel at

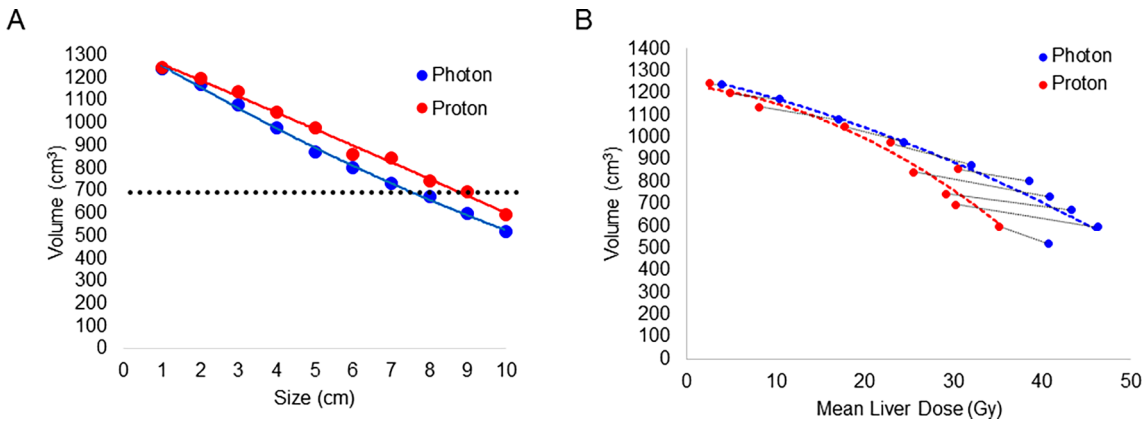

Fig. 1. Target size and its impact on the ability to meet liver constraints for lesions located in the dome. (A) Liver volume receiving < 15 Gy (y axis) as a function of target diameter (x axis). Horizontal dotted line represents the standard constraint of 700 cm^3. Protons plans met constraints up to 9 cm whereas photon plans met constraints only up to 7 cm. (B) Comparison of volume receiving < 15 Gy (y axis) and mean liver dose expressed in LQED2 (x axis), two parameters known to impact liver toxicity. Black dotted lines represent paired photon-proton plans per size. Colored dash lined represent trend. Compared to photon plans, proton plans showed a reduction in mean liver dose even in plans that had similar volume receiving < 15 Gy.

Table 4
Additional liver sparing with protons.

Position	V < 15 Gy (cm^3)	MLD (Gy)	MLD (LQED2) (Gy)	NTCP (%)
Dome*	68 ± 11	-3.5 ± 0.6	-9.1 ± 1.5	-0.36 ± 0.13
Right inferior*	54 ± 13	-2.3 ± 0.6	-6.0 ± 1.7	-0.12 ± 0.06
Left medial*	70 ± 13	-3.1 ± 0.4	-8.1 ± 1.0	-0.02 ± 0.01
Central*	45 ± 10	-2.7 ± 0.4	-7.1 ± 1.1	-0.17 ± 0.06
Average	59 ± 6	-2.9 ± 0.3	-7.5 ± 0.7	-0.17 ± 0.07

Values represent averaged difference (proton minus photon) across all sizes ± standard error. MLD = mean liver dose, LQED2 = equivalent dose in 2 Gy fractions, NTCP = normal tissue complication probability. *p < 0.01 for all comparisons.

target diameters 8–10 cm, while photons violated both the point and volumetric constraints (20 cm^3 < 25 Gy) at the same target sizes.

While protons have higher entrance dose compared to photons, there were no substantial or clinically meaningful differences between the skin and chest wall dose comparing SBPT and SBRT. SBRT met skin constraints for larger targets in position B, but was more limited than SBPT for targets in position C. Additionally, SBPT met chest wall constraints for larger targets than SBRT in positions B and C (8 cm v. 6 cm, Supplement B).

4. Discussion

We evaluated the theoretical dosimetric advantages of proton SBRT (SBPT) for liver tumors up to 10 cm diameter at four different locations. We demonstrate that compared to photon SBRT, SBPT can generally deliver a higher dose to the target volume and better spare OARs, thus achieving two often mutually-exclusive theoretical advantages: potential for improved local control and toxicity reduction. We also find that SBPT may be particularly beneficial for larger target volumes that would not otherwise be targetable using SBRT (without compromising target dose). This is in agreement with data from a recent study of proton SBRT for liver metastases (up to 11.9 cm) demonstrating good efficacy (> 75% local control at 1 year) without any grade 3–5 toxicities [22]. Additionally, a randomized phase III trial recently opened comparing proton to photon SBRT for hepatocellular carcinoma (NRG-GI003 [NCT03186898]), which aims to evaluate whether SBPT is superior to SBRT, specifically looking at overall survival.

Given the inherent sensitivity of the liver to radiation, maximizing liver sparing is a critical objective in SBRT planning and is often the limiting constraint, particularly for larger target sizes. We find that SBPT could spare larger volumes of uninvolved liver from radiation with a lower liver NTCP, even at times when established volumetric liver constraints were not met. Petersen et al. [13] reported their dosimetric findings comparing SBRT to SBPT for target volumes 25–232 cm^3, and found as we did that proton-based therapy can substantially reduce dose to the uninvolved liver (median 9.1 Gy vs. 20.0 Gy; $p < 0.005$). Toramatsu and colleagues applied an NTCP model similar to ours and showed that for target diameters > 6.3 cm, SBPT substantially lowed the estimated risk of RILD compared to SBRT (94.5% for SBRT and 6.2% for SBPT) [14]. Thus, the liver-sparing advantage with proton-based SBRT could potentially be most beneficial to patients with advanced cirrhosis, who have higher rates of radiation-induced liver disease (RILD) after photon SBRT (20–50%) [23–26].

In addition to target size, the dosimetric advantages seen in SBPT are also dependent upon target location. For instance, protons exhibited no dosimetric advantage in the left medial location (correlating roughly to segment 4 in the liver, position C as discussed in this study), as both SBPT and SBRT were limited at 6 cm size by duodenum constraints (as well as stomach in proton plans) without any anticipated reduction in liver NTCP (Fig. 2C). In other locations (dome, right medial and central; correlating to segments 8, 6, and 5, respectively), there was a clear advantage of SBPT in both maximizing GTV dose and limiting dose to OARs, especially for larger target diameters ≥ 6 cm (e.g. Fig. 2A and B). Of note, to achieve this improvement, an increasing number of beams was required to decrease the skin and chest wall dose due to higher entry dose. These results confirm other work demonstrating both location and size dependence of SBPT benefit for small target volumes (≤ 6 cm) [27]. However, here we demonstrate that proton's main advantage may be for larger target volumes, enabling SBRT that would otherwise not be deliverable without compromising prescription dose.

We note that there are several limitations to this study. Given these are theoretical treatment volumes that are concentrically expanded and cropped to the existing liver contour, the volumes themselves may not reflect target shape in an actual patient. Nor did we study anatomical variability in liver size or shape or varying duodenum/bowel positions. However, our approach enabled a standardized comparison that allows generalization and the conclusions we draw should apply to the majority of patients seen in practice. Certainly, there could be planning limitations with irregularly shaped targets that could limit planning using any modality. In addition, the NTCP model used in this study was generated from photon-based data, and it is possible this model would have to be modified for proton therapy. However, such model is not yet available. These limitation notwithstanding, the methodology used in this study does allow us to draw general conclusions that would be helpful in selecting patients most suitable for SBPT.

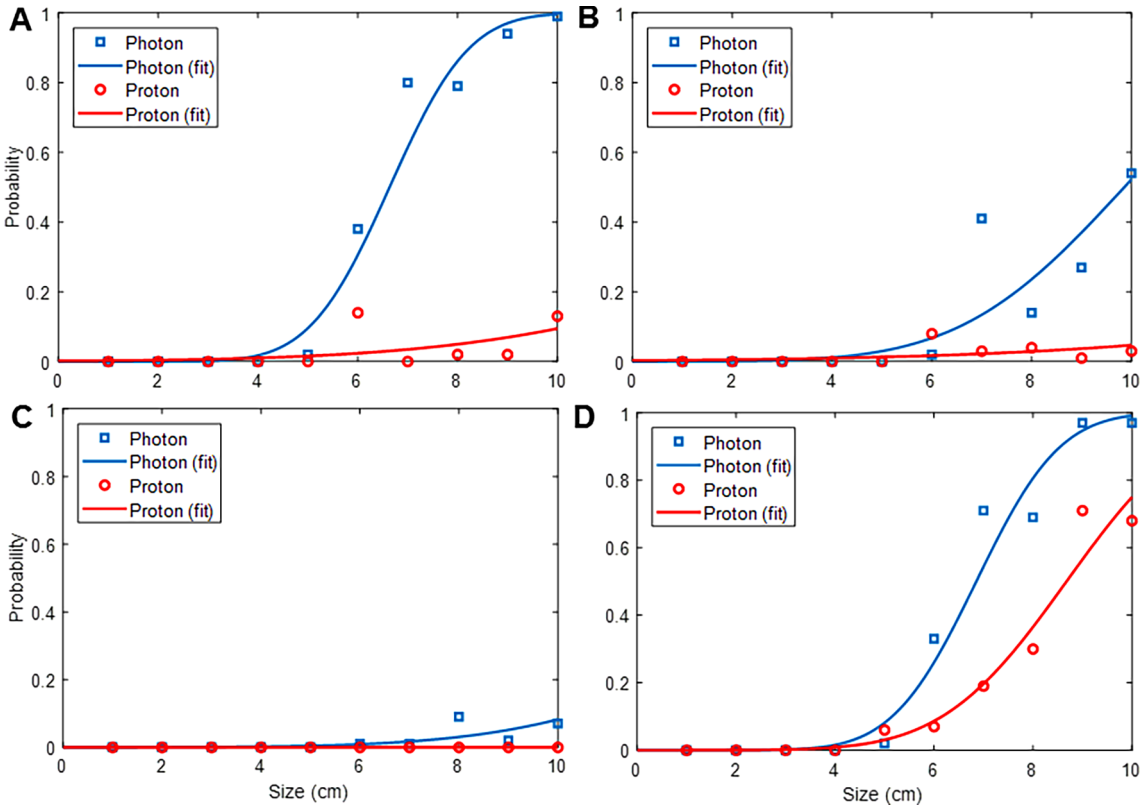

Fig. 2. Evaluation of liver NTCP in photon and proton plans in each corresponding location in the liver. NTCP was computed using the Lyman-Kutcher-Burman model, applied to biologically-corrected DVH data. X axis shows target diameter; Y axis shows NTCP values. A, dome; B, right inferior; C, left medial; D, central. Proton plans resulted in lower NTCP than photon plans, which was most pronounced for targets in the dome.

Finally, we did not take into account target motion in the current study. We recognize that motion can degrade the dose distribution of both proton and photon SBRT, but assume that in any clinical implementation motion management will be addressed with established effective methods. In this work, we selected proton beam angles that traverse anatomy that is least likely to change day-to-day or with organ motion. Motion mitigation techniques such as the use of a compression belt or breath hold during treatment would further reduce the impact of motion on the delivered dose distribution. Studies have demonstrated that 3–5 repaintings in PBS delivery is sufficient to minimize the interplay effect in liver tumors [28], and this methodology could be applied in liver proton SBRT.

The current study demonstrated that proton-based SBRT for liver tumors could achieve a higher dose to targets than photons while sparing OARs at least as well as photon-based plans. This effect was seen across all target sizes, but it was more pronounced in larger-sized lesions. Proton SBRT could better spare the uninvolved liver, particularly for targets in the dome and central locations. In contrast, targets located in the left medial and right inferior locations, limited by adjacent small bowel/duodenum, were generally equally well treated with photons. Given the theoretical dosimetric and radiobiological advantages we have observed in this study, we are proceeding with a prospective clinical trial of proton SBRT for patients with large hepatic lesions.

Conflicts of interest

None.

Appendix A. Supplementary data

Supplementary data to this article can be found online at https://doi.org/10.1016/j.phro.2018.11.004.

References

[1] Bujold A, Massey CA, Kim JJ, Brierley J, Cho C, Wong RK, et al. Sequential phase I and II trials of stereotactic body radiotherapy for locally advanced hepatocellular carcinoma. J Clin Oncol. 2013;31:1631–9.
[2] Barry A, McPartlin A, Lindsay P, Wang L, Brierley J, Kim J, et al. Dosimetric analysis of liver toxicity after liver metastasis stereotactic body radiation therapy. Pract Radiat Oncol. 2017.
[3] Swaminath A, Massey C, Brierley JD, Dinniwell R, Wong R, Kim JJ, et al. Accumulated Delivered Dose Response of Stereotactic Body Radiation Therapy for Liver Metastases. Int J Radiat Oncol Biol Phys. 2015;93:639–48.
[4] Sapisochin G, Barry A, Doherty M, Fischer S, Goldaracena N, Rosales R, et al. Stereotactic body radiotherapy vs. TACE or RFA as a bridge to transplant in patients with hepatocellular carcinoma. An intention-to-treat analysis. J Hepatol. 2017;67:92–9.
[5] Hong JC, Salama JK. The expanding role of stereotactic body radiation therapy in oligometastatic solid tumors: What do we know and where are we going? Cancer Treat Rev. 2017;52:22–32.
[6] Eccles CL, Bissonnette JP, Craig T, Taremi M, Wu X, Dawson LA. Treatment planning study to determine potential benefit of intensity-modulated radiotherapy versus conformal radiotherapy for unresectable hepatic malignancies. Int J Radiat Oncol Biol Phys. 2008;72:582–8.
[7] Thomas E, Chapet O, Kessler ML, Lawrence TS, Ten Haken RK. Benefit of using biologic parameters (EUD and NTCP) in IMRT optimization for treatment of intrahepatic tumors. Int J Radiat Oncol Biol Phys. 2005;62:571–8.
[8] Tsai YC, Tsai CL, Hsu FM, Jian-Kuen W, Chien-Jang W, Cheng JC. Superior liver sparing by combined coplanar/noncoplanar volumetric-modulated arc therapy for hepatocellular carcinoma: a planning and feasibility study. Med Dosim. 2013;38:366–71.
[9] Scorsetti M, Comito T, Cozzi L, Clerici E, Tozzi A, Franzese C, et al. The challenge of inoperable hepatocellular carcinoma (HCC): results of a single-institutional experience on stereotactic body radiation therapy (SBRT). J Cancer Res Clin Oncol. 2015;141:1301–9.

[10] Ben-Josef E, Normolle D, Ensminger WD, Walker S, Tatro D, Ten Haken RK, et al. Phase II trial of high-dose conformal radiation therapy with concurrent hepatic artery floxuridine for unresectable intrahepatic malignancies. J Clin Oncol. 2005;23:8739–47.
[11] Seong J, Park HC, Han KH, Chon CY. Clinical results and prognostic factors in radiotherapy for unresectable hepatocellular carcinoma: a retrospective study of 158 patients. Int J Radiat Oncol Biol Phys. 2003;55:329–36.
[12] Hong TS, Wo JY, Yeap BY, Ben-Josef E, McDonnell EI, Blaszkowsky LS, et al. Multi-Institutional Phase II Study of High-Dose Hypofractionated Proton Beam Therapy in Patients With Localized, Unresectable Hepatocellular Carcinoma and Intrahepatic Cholangiocarcinoma. J Clin Oncol. 2016;34:460–8.
[13] Petersen JB, Lassen Y, Hansen AT, Muren LP, Grau C, Hoyer M. Normal liver tissue sparing by intensity-modulated proton stereotactic body radiotherapy for solitary liver tumours. Acta Oncol. 2011;50:823–8.
[14] Toramatsu C, Katoh N, Shimizu S, Nihongi H, Matsuura T, Takao S, et al. What is the appropriate size criterion for proton radiotherapy for hepatocellular carcinoma? A dosimetric comparison of spot-scanning proton therapy versus intensity-modulated radiation therapy. Radiat Oncol. 2013;8:48.
[15] Weiner AA, Olsen J, Ma D, Dyk P, DeWees T, Myerson RJ, et al. Stereotactic body radiotherapy for primary hepatic malignancies - Report of a phase I/II institutional study. Radiother Oncol. 2016;121:79–85.
[16] Scorsetti M, Comito T, Tozzi A, Navarria P, Fogliata A, Clerici E, et al. Final results of a phase II trial for stereotactic body radiation therapy for patients with inoperable liver metastases from colorectal cancer. J Cancer Res Clin Oncol. 2015;141:543–53.
[17] Goodman KA, Wiegner EA, Maturen KE, Zhang Z, Mo Q, Yang G, et al. Dose-escalation study of single-fraction stereotactic body radiotherapy for liver malignancies. Int J Radiat Oncol Biol Phys. 2010;78:486–93.
[18] Su TS, Lu HZ, Cheng T, Zhou Y, Huang Y, Gao YC, et al. Long-term survival analysis in combined transarterial embolization and stereotactic body radiation therapy versus stereotactic body radiation monotherapy for unresectable hepatocellular carcinoma > 5 cm. BMC Cancer. 2016;16:834.
[19] Thompson R. RadOnc: an R package for analysis of dose-volume histogram and three-dimensional structural data. J Radiat Oncol Inform. 2014;6:98–110.
[20] Spalding AC, Jee KW, Vineberg K, Jablonowski M, Fraass BA, Pan CC, et al. Potential for dose-escalation and reduction of risk in pancreatic cancer using IMRT optimization with lexicographic ordering and gEUD-based cost functions. Med Phys. 2007;34:521–9.
[21] Velec M, Haddad CR, Craig T, Wang L, Lindsay P, Brierley J, et al. Predictors of Liver Toxicity Following Stereotactic Body Radiation Therapy for Hepatocellular Carcinoma. Int J Radiat Oncol Biol Phys. 2017;97:939–46.
[22] Hong TS, Wo JY, Borger DR, Yeap BY, McDonnell EI, Willers H, et al. Phase II Study of Proton-Based Stereotactic Body Radiation Therapy for Liver Metastases: Importance of Tumor Genotype. J Natl Cancer Inst. 2017;109.
[23] Culleton S, Jiang H, Haddad CR, Kim J, Brierley J, Brade A, et al. Outcomes following definitive stereotactic body radiotherapy for patients with Child-Pugh B or C hepatocellular carcinoma. Radiother Oncol. 2014;111:412–7.
[24] Jung J, Yoon SM, Kim SY, Cho B, Park JH, Kim SS, et al. Radiation-induced liver disease after stereotactic body radiotherapy for small hepatocellular carcinoma: clinical and dose-volumetric parameters. Radiat Oncol. 2013;8:249.
[25] Ohri N, Jackson A, Mendez Romero A, Miften M, Ten Haken RK, Dawson LA, et al. Local Control Following Stereotactic Body Radiotherapy for Liver Tumors: A Preliminary Report of the AAPM Working Group for SBRT. Int J Radiat Oncol Biol Phys. 2014;90:S52.
[26] Cardenes HR, Price TR, Perkins SM, Maluccio M, Kwo P, Breen TE, et al. Phase I feasibility trial of stereotactic body radiation therapy for primary hepatocellular carcinoma. Clin Transl Oncol. 2010;12:218–25.
[27] Gandhi SJ, Liang X, Ding X, Zhu TC, Ben-Josef E, Plastaras JP, et al. Clinical decision tool for optimal delivery of liver stereotactic body radiation therapy: photons versus protons. Pract Radiat Oncol. 2015;5:209–18.
[28] Lin L, Souris K, Kang M, Glick A, Lin H, Huang S, et al. Evaluation of motion mitigation using abdominal compression in the clinical implementation of pencil beam scanning proton therapy of liver tumors. Med Phys. 2017;44:703–12.